Food Research International 208 (2025) 116248

Contents lists available at ScienceDirect

Food Research International

journal homepage: www.elsevier.com/locate/foodres

Effect of β-glucan on the gelling properties of unwashed silver carp surimi gel: Insights into molecular interactions between different sources of β-glucan and myofibrillar protein

Yisha Xie [a,*,1], Kangyu Zhao [a,1], Jing Peng [a], Li Jiang [a], Wenjing Shu [a], Yizhen Huang [b], Qingqing Liu [a], Wei Luo [c], Yongjun Yuan [a,*]

[a] Food Microbiology Key Laboratory of Sichuan Province, Chongqing Key Laboratory of Speciality Food Co-Built by Sichuan and Chongqing, School of Food and Bioengineering, Xihua University, Chengdu 610039, Sichuan, China
[b] College of Food Science and Nutritional Engineering, China Agricultural University, Beijing 100083, China
[c] College of Biological Science and Engineering, Fuzhou University, Fuzhou 350108, Fujian Province, China

ARTICLE INFO

Keywords:
Protein
β-Glucan
Gel characteristic
Structure

ABSTRACT

Gel property is one of the most important abilities to surimi products. In this research, the β-glucan from yeast and oat were applied in enhancing the gel properties of unwashed surimi gel. The texture profile analysis (TPA), storage modulus (*G'*), loss modulus (*G''*) of unwashed surimi gel, and β-glucan linking with myofibrillar protein were investigated, at the addition of 0 %–1.5 % β-glucan. The β-glucan from yeast and oat could induce more unfolding and promoted cross-linking of myofibrillar protein, improving the hardness and gel strength of unwashed surimi gel. At the 1.0 % addition of yeast β-glucan (YG) or oat β-glucan (OG), the gel strength of unwashed surimi gel increased by 434.30 g·mm and 314.39 g·mm, respectively, compared with the control. In addition, YG with a branched-chain structure was more likely to crosslink with myofibrillar protein (MHC) through hydrogen bond, and YG-MHC CDOCKER energy lower than OG-MHC, proved by molecular docking analysis. The grafting degree and intermolecular interactions in the YG treated surimi gel are stronger than those in the OG one, enhancing the physical properties and WHC of unwashed surimi gel. However, as the added amount β-glucan increased 1.5 %, the pores in the network became excessively expansive, the continuous structure of the myofibrillar protein was gradually destroyed, leading to the decreasing gel properties and rheological properties. In conclusion, 1.0 % YG treatment can effectively improve the gel properties of unwashed surimi gel, providing a practical method for the processing of myofibrillar protein based gel products.

1. Introduction

The nutritional value and delicate taste of silver carp make it a key ingredient in the creation of surimi-based products, highlighting its significance in both commercial and consumer markets (Walayat, Wei, Su, Lorenzo, & Nawaz, 2024). Unwashed surimi gel retains all the nutrients such as water-soluble proteins of the whole fish, and alleviating the process complexity and waste water disposal (Gore et al., 2022; Shen et al., 2022), yet it has lower gel strength compared to washed surimi gel. The interaction between polysaccharides and proteins usually effectively adjusting the gel properties, the preparation and characterization of the composite gels have been studied extensively (S. Li et al., 2024; Zhuang, Wang, Jiang, Chen, & Zhou, 2021). There are other substances that have been reported to enhance the gelation properties (Zhang et al., 2024; Zhang et al., 2025). Several polysaccharides have been successfully applied to surimi products derived from freshwater fish, including okra polysaccharide, β-glucans, chitosan, konjac glucomannan and carboxymethyl cellulose sodium (He et al., 2023; S. Li et al., 2024; X. Wang et al., 2024). Huo, Wuhanqimuge, Zhang, Sun and Miao (2025) investigated β-glucan with diverse conformations docking with the Dectin-1 protein, and found the interaction range between Dectin-1 and high-polymerization triple-helix β-glucans followed the order: type 2 (single-chain model with high polymerization) > type 1 (single-chain model with low polymerization) > type 3 (parallel three-chain model

* Corresponding authors.
E-mail addresses: Isabella-xie@foxmail.com (Y. Xie), yyja9791@sina.com (Y. Yuan).
[1] Yisha Xie and Kangyu Zhao contributed equally to this work.

https://doi.org/10.1016/j.foodres.2025.116248
Received 17 December 2024; Received in revised form 18 February 2025; Accepted 11 March 2025
Available online 15 March 2025

with high polymerization).

β-glucans are large, complex sugar molecules made up of D-glucose units connected by β-glycosidic bonds, and they are prevalent in both plants and microorganisms (Bai et al., 2019). The structures of β-glucan vary according to different sources. The microbial β-glucans have short β-(1 → 6)-linked branches from a β-(1 → 3) backbone. The β-glucans of oats and barley are linear β-(1 → 4) linkages separating shorter chain of β-(1 → 3) structures (Sujithra, Arthanareeswaran, Ismail, & Taweepreda, 2024). The differences in the chemical structure of the β-glucans likely affect biological activities. It has been reported that β-glucans with β-(1 → 3)-linkages associated to β-(1 → 6) branches possess strong immune action and proved to have higher proinflammatory cytokine stimulation (Jayachandran, Chen, Chung, & Xu, 2018; Vannucci et al., 2013). As the main cereal source of β-glucan, oat β-glucan (OG) exhibited superior water absorption ability during cooking, which contributed to a tender and succulent texture in meat products (Liu, Wang, Li, & Zhang, 2015). One of the new resource foods, yeast cell walls containing β-glucan, which has a high viscosity, water-holding, and emulsion stabilizing capacities, effectively improving the texture and sensory properties of low-fat food. Researches have shown that a proper addition of yeast β-glucan (YG) significantly improved WHC and gel strength of surimi gels (Zhang et al., 2019). The addition of 0 %–1 % OG resulted in a homogeneous gel network structure and enhanced gel properties of surimi (He et al., 2023). However, the mechanism by which the molecular structure and source of β-glucan regulate the quality of the gel is still unclear.

Ultrasound has garnered extensive application in protein gel fields, including surimi, due to non-pollution, safety, and ease of operation. Our previous work revealed that ultrasound-assisted first-stage thermal treatment (UATT) was a promising method to improve the gel quality of unwashed surimi gel (Xie et al., 2024). However, the strengthening effect of gelation under UATT, in combination with other food components like β-glucans, remains unclear. Through literature search and preliminary experiments, the addition amount of β-glucan was determined to be 0 %–1.5 % (He et al., 2023; Xie, Zhao, et al., 2024). The influence of YG or OG at different contents (0 % - 1.5 %) on the gel properties (texture, water holding capacity, *etc.*) of unwashed surimi gel was investigated, under UATT treatment. The interactions between β-glucan and myofibrillar protein were analyzed through determining fluorescence, grafting degree, combining with molecular docking. This comprehensive study revealed the mechanism of β-glucan from yeast and oats enhances gel-related properties, providing the theoretical foundation for the effective use of β-glucan in protein gel.

2. Materials and methods

2.1. Materials

The fresh Silver Carp (*Hypophthalmichthys molitrix*) was purchased from local market (Chengdu, China) in February to June. The YG (food grade, purity of 80 %, ~50,000 Da, the degree of polymerization: 125 to 25,000) and OG (food grade, purity of 80 %, ~1000 Da, the degree of polymerization: 10 to 3000) were purchased from Xi'an Shengqing Biotechnology Co., Ltd. and Guangzhou Yizhilai Biotechnology Co., Ltd., respectively. NaCl was purchased from Tianjin Zhiyuan Chemical Reagent Co., Ltd. (China). Urea was purchased from Sangon Biotech (Shanghai) Co., Ltd. (China). β-mercaptoethanol was purchased from Chengdu Kelong Chemical Co., Ltd. (China). Nile blue and calcofluor white were purchased from Shanghai Macklin Biochemical Co., Ltd. and Sigma Aldrich (Shanghai) Trading Co., Ltd. (China), respectively. O-phthalaldehyde (OPA) was purchased from Shanghai Aladdin Biochemical Technology Co., Ltd. (China).

2.2. Preparation of unwashed silver carp surimi gels with β-glucan

The preparation of Silver Carp surimi gel was similar to previous work (Xie, Zhao, et al., 2024). Live silver carp (average weight 1.5 ± 0.06 kg) was sacrificed, and the head knocking, a non-stressful method, was used to stunning the fish (Zhang et al., 2023). The descaled fish placed in an ice bath box was quickly transported to the laboratory in 30 min. The dorsum muscle of Silver Carp fish (about 300 g) was collected and ground at the second gear for 2 min (stop every 30 s) in the ice water bath with a grinder (OLK-JR01, OLAYKS, Zhongshan, China), with 1.5 % (*w/w*) NaCl and 0 %–1.5 % (*w/w*) YG or OG. The water content of surimi was about 18 %, tested by a Moisture Analyzer (MA35M-1CN230V1, Sartorius, Germany). The samples were transferred into the water bath at 40 °C for 30 min assistance with the ultrasound treatment (SB-5200DTN, ultrasonic cleaners, 300 W, 40 kHz, Xinzhi, Ningbo, China), obtaining a set of sol samples. The ultrasonic treatment parameters were determined by our previous work (Xie, Zhao, et al., 2024). Finally, all sol samples were placed in 90 °C water for 30 min, and a set of surimi gel samples obtained. The process flow diagram and visual appearance as shown in Fig. 1.

2.3. Physical property analysis

2.3.1. Gel strength

By methodology of Xie, Zhao, et al. (2024), the gel strength of gel samples was determined by a TA-XT-Plus texture analyzer (Stable Micro Systems Ltd., Godalming, UK) with the P/2 probe at a pretest speed, 2.0 mm/s; test speed, 1.0 mm/s; post-test speed, 10.0 mm/s. The compression distance was 5.0 mm and 10 g of trigger force. The experiment was repeated twelve times.

2.3.2. Texture profile analysis (TPA)

The TPA of surimi gels was assayed according to Xie, Zhao, et al. (2024) with some alteration. Cylindrical gel samples (height = 2.0 cm, diameter = 2.0 cm) were placed on the TA-XT-Plus texture analyzer (Stable Micro Systems Ltd., Godalming, UK) and measured at the trigger force of 10 g, with the P/36R probe (cylindrical probe, 36 mm in diameter). The pretest, test, and post-test speeds were set as 5.0 mm/s, 3.0 mm/s, and 3.0 mm/s, respectively, with 40 % of strain. The hardness, springiness, cohesiveness, and chewiness of surimi gels were recorded. The experiment was repeated five times.

2.3.3. Rheological measurement

The rheological behavior of surimi gels with 0 %–1.5 % YG and OG was investigated using a Rotational Rheometer (MCR302, Anton Paar, Austria). The method is similar to the previous study (Xie, Zhao, et al., 2024), the storage modulus (G') and loss modulus (G'') of the sol sample with heating and cooling was measured in the range of 10 rad/s, and 0.01 % of strain. The temperature gradient was set as 40 °C to 90 °C at a heating rate of 3 °C/min, after maintaining for 15 min, decreasing from 90 °C to 25 °C at a cooling rate of 1 °C/min.

2.4. The water retention characterization

2.4.1. Determination of water holding capacity (WHC)

The WHC was determined by the methodology of He et al. (2023). The surimi gels were sliced into thin blocks and then weighed (denoted C_1). Subsequently, the weight of samples after centrifugation (986.076 ×*g* for 20 min at 25 °C) was denoted as C_2, and the WHC was calculated as follows:

$$\mathrm{WHC}(\%) = C_2/C_1 \times 100 \quad (1)$$

2.4.2. Low-field nuclear magnetic resonance (LF-NMR)

Relaxation time (T_2) was determined by low-field NMR according to the method of Zhang et al. (2019) with a slight modification. Briefly, approximately 5 g of gel sample was put into the cylindrical glass tubes. The T_2 was evaluated on an LF-NMR analyzer (Niumag Analytical Instruments, China) operating at 21 MHz and 32 °C. The test parameters

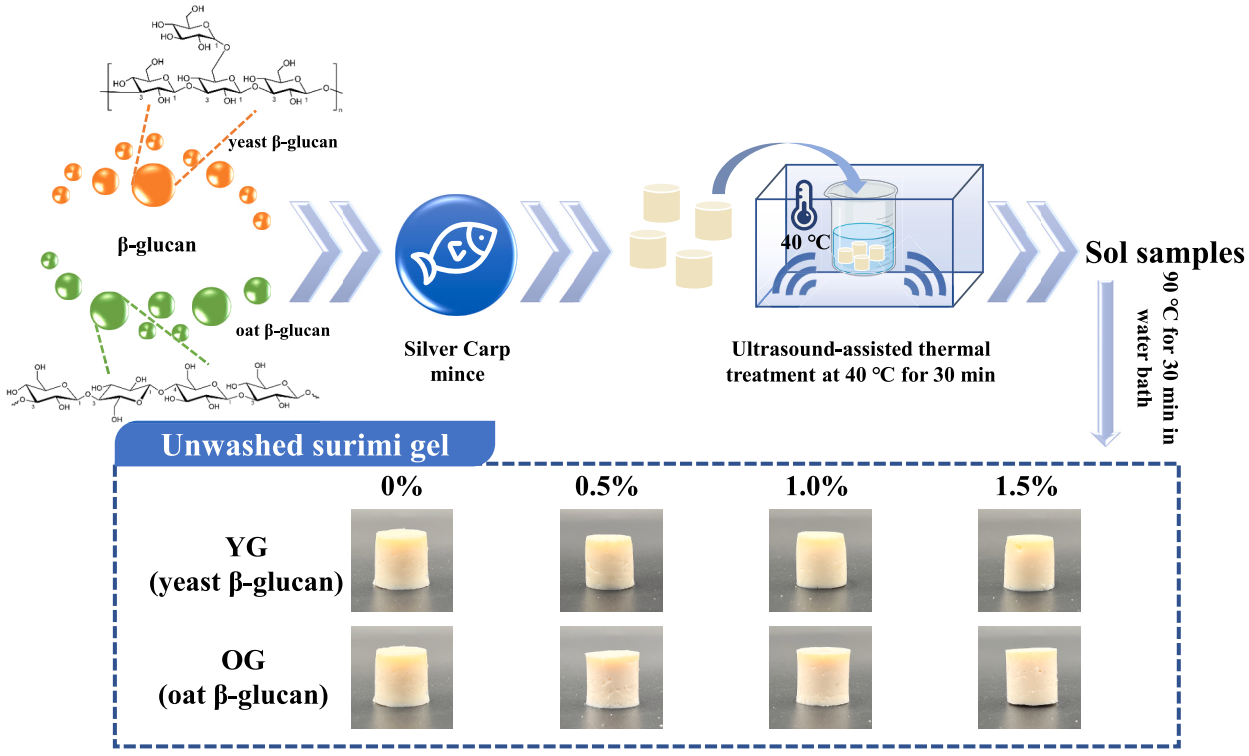

Fig. 1. The process flow diagram and visual appearance of surimi gels with YG or OG.
Note: YG - the surimi gel with yeast β-glucan, OG - the surimi gel with oat β-glucan.

were set as follows: SW = 100 kHz, TW = 3000 ms, P1 = 10.00 μs, P2 = 20.48 μs, NS = 4, TE = 0.4 ms, NECH = 5000. Finally, the low-field NMR curves that reflected water distribution and the proportion of bound water (T_{21}), immobile water (T_{22}), and free water (T_{23}) were obtained.

2.5. Preparation of myofibrillar protein - β-glucan solution

To analyze the impact of β-glucan from different sources on the structure of myofibrillar protein. The myofibrillar protein was extracted from Silver Carp following the method in previous report (Xie, Zhao, et al., 2024), and mixed with YG or OG based on the ratio of dry matter in surimi to β-glucan. The specific mixing ratios were as follows: 2 g of extracted myofibrillar protein was mixed with 0.0066 g of NaCl, and then 0.0022 g, 0.0044 g, or 0.0066 g of YG or OG were added, respectively. The mixtures were homogenized on a vortex oscillator (Vortex Genius 3, IKA/Germany) and then subjected to thermal treatment according to Section 2.2, and stored at 4 °C for the grafting degree and spectral analysis.

2.6. Grafting degree (GD) analysis

The degree of glycosylation was ascertained using the o-phthalaldehyde (OPA) method, with certain modifications as detailed by Geng et al. (2024). Briefly, 80 mg of o-phthalaldehyde (OPA) was dissolved in 2 mL of the ethanol solution. Meanwhile, 3.81 g of sodium tetraborate decahydrate, 0.1 g of sodium dodecyl sulfate (SDS), and 88 mg of DL-Dithiothreitol (DTT) were completely dissolved in 75 mL of deionized water. The OPA reagent was prepared by combining the ethanol solution with the aqueous solution, and diluted to a final volume of 100 mL with deionized water. Thereafter, 200 μL of a 5 mg/mL protein solution was thoroughly mixed with 4 mL of the prepared OPA reagent, and the mixture was incubated in the dark for 10 min at ambient temperature. The absorbance of each sample was registered at 340 nm using a UV-1900 spectrophotometer (Shimadzu Inc., Kyoto, Japan). PBS was used as the blank control. The DG (%) was calculated by eq. (2):

$$DG = (D_0 - D_1)/D_0 \times 100\% \quad (2)$$

Where D_0 and D_1 are the absorbance of the solution before and after glycosylation, respectively.

2.7. Intrinsic fluorescence spectrum

The intrinsic fluorescence emission spectra were recorded by using a fluor photometer (FluoroMax-4, HORIBA, Japan) based on the method by Xie, Zhao, et al. (2024). The concentration of the protein solution was diluted to 0.5 mg/mL. Subsequently, the excitation wavelength was adjusted to 285 nm, and the slit width was set at 5 nm. The fluorescence spectrum was then scanned over an emission wavelength range of 305–500 nm at a temperature of 25 °C.

2.8. Secondary structure analysis

The secondary structures of myofibrillar protein were measured in the far-ultraviolet region (190–260 nm), using a spectropolarimeter (Chirascan qCD, Applied Optical Physics, UK) (Xie, Zhao, et al., 2024). The concentration of the protein solution was adjusted to 1 mg/mL in a 1 mm quartz cuvette, analyzed by the CDNN software (version 2.1, Applied Photophysics, Leatherhead, Surrey, UK, 2011).

2.9. Raman spectroscopy

Raman spectra of gels were tested using a Raman spectrometer (DeepBlue2000, HORIBA Scientific, Japan) according to the method reported by Mi et al. (2021), at 25 °C in the range of 400–3600 cm^{-1} with a 532 nm laser source, 100 mW laser power, 2.0 cm^{-1} spectral resolution and exposure time of 40 s. The spectra were smoothed, baseline-corrected, and normalized using phenylalanine at 1003 cm^{-1}. Raman peaks at 830 cm^{-1} and 850 cm^{-1} are correlated to two types of hydrogen bonds: “exposed” tyrosine and “buried” tyrosine, which can be quantified by solving Eqs. (3) and (4) (Xie et al., 2022):

$$N_{buried} + N_{exposed} = 100\% \quad (3)$$

$$0.5\ N_{buried} + 1.25\ N_{exposed} = I_{850}/I_{830} \quad (4)$$

Where N_{buried} is the molar fraction of "buried" tyrosine residues, $N_{exposed}$ is the molar fraction of "exposed" tyrosine residues.

2.10. Measurement of intermolecular interactions

The solubility of proteins was determined by different chemical reagents that could destroy the internal chemical forces of molecules: 0.6 mol/L NaCl for breaking electrostatic force and hydrogen bonds, 1.5 mol/L urea for breaking hydrogen bonds, 8 mol/L urea for breaking hydrogen bonds and hydrophobic interactions, 0.5 mol/L β-mercaptoethanol for breaking disulfide bond (Yuan et al., 2019). Surimi gel samples (4 g) were added to 20 mL of 0.05 mol/L NaCl solution (S_1), 0.6 mol/L NaCl solution (S_2), 1.5 mol/L urea +0.6 mol/L NaCl solution (S_3), 8 mol/L urea +0.6 mol/L NaCl solution (S_4), and 0.6 mol/L NaCl +8 mol/L urea +0.5 mol/L β-mercaptoethanol (S_5) (Mi et al., 2021). The mixture was homogenized using a high-speed disperser (FSH-2 A, Changzhou Jintan Liangyou Instrument Co., Ltd., China) at 10956.40 ×g for 2 min and left to stand for 1 h at 4 °C. Subsequently, the mixture was centrifuged at 8000 r/min for 15 min in a freezing centrifuge (GL-20G-II, Shanghai Anting Scientific Instrument Factory). The protein content of the supernatant was measured following the procedure used by Bradford. The formulas for calculating chemical forces are shown as follows:

$$\textit{Ionic bonds} = c\ (S_2 - S_1) \quad (5)$$

$$\textit{Hydrogen bonds} = c\ (S_3 - S_2) \quad (6)$$

$$\textit{Hydrophobic interactions} = c\ (S_4 - S_3) \quad (7)$$

$$\text{Disulfide bonds} = c\ (S_5 - S_4) \quad (8)$$

2.11. Molecular docking

The myosin heavy chain (MHC) II A structure of *Hypophthalmichthys molitrix* (the PDB ID 1YV3, referring to Li et al. (2021)) was selected. The structures of two kinds of β-glucan were referred from Rahar, Swami, Nagpal, Nagpal, and Singh (2011). The β-glucan ligands were prepared (pH 7.0) and performed energy minimization settings after being imported into the DS software. Then, the myosin heavy chain II A structure and β-glucan monomer were treated by the CHARMM force field. Then the CDOCKER protocol was used for molecular docking between MHC and β-glucans.

2.12. Microstructure characterization

2.12.1. Light microscopy with Harris-eosin (HE) staining

The spatial distribution of protein in the surimi gels was examined under light microscopy following HE staining. Hubei BIOSSCI Biotech Co., Ltd. (Wuhan Changyan Pathology Technology Co., Ltd.) offered technical assistance for the preparation of paraffin sections and the HE staining process. Briefly, the fixed structure of surimi gels was dehydrated by sequential immersion in a graded ethanol series and xylene, prior to being embedded in paraffin. A serial section 4 μm thick was conducted using a microtome (SHANDON FINESSE325, Thermo Fisher Scientific Co., Ltd., USA), de-paraffin with clearer (Wuhan Tongsheng Technology Development Co., Ltd.) and absolute ethyl alcohol. The deparaffined section was stained hematoxylin solution (Harris) for 4 min and then washed with tap water, stained again with eosin solution (alcohol soluble) for 20 s. After being treated with 95 % ethanol for 5 min, the tissue sections were transparent with xylene and then mounted with neutral balsam. The distribution of myofibrillar protein in the surimi gels is pink to red, observed under 40× and 100× optical microscope (B302, Chongqing Optec Instrument Co., Ltd., China).

2.12.2. Confocal laser scanning microscopy (CLSM)

The distribution of β-glucan and protein in the surimi gels was evaluated using a confocal laser scanning microscope (CLSM). Nile blue (0.1 %, *w/v,* in water) and calcofluor white (0.01 %, *v/v*, in water) were used as fluorescence dyes for the proteins and polysaccharides, respectively. The thinly layered surimi gel sample was immersed in a 4 mL dye mixture (2 mL of Nile blue solution, and 2 mL of calcofluor white solution), and then the mixture heated to 90 °C for 5 min, protected from light. The stained samples were mounted on slides and secured with coverslips for microscopic examination, with β-glucan in blue and proteins in green. The excitation wavelengths of Nile blue and calcofluor white were 638 nm and 405 nm, respectively (Yang et al., 2022). The photographs were captured using a CLSM600 equipment (Ningbo Sunny Instruments Co., Ltd. Ningbo, China).

2.12.3. Scanning electron microscope (SEM)

The scanning electron microscopy (SEM) was used to observe the microstructures of the surimi gel samples following the report of Xie, Zhao, et al. (2024). Briefly, the platinum was applied to each lyophilized surimi gel after it had been mounted on a bronze stub (thickness: 5 nm, EM ACE200, Leica, Germany). The microstructure of surimi gels was observed under 500× and 1000× magnification by SEM (Quattro ESEM, Thermo Fisher Scientific Co., Ltd., USA). The average pore size was calculated by transforming SEM images into the public software ImageJ 1.53a (National Institutes of Health, Bethesda, MD, USA), according to the method reported by Dàvila, Toldrà, Saguer, Carretero, and Parés (2007).

2.13. Statistical analysis

All experimental data were set up in triplicate, unless specified otherwise. The data was analyzed utilizing SPSS software (IBM SPSS Statistics version 26), with mean comparisons performed using the Least Significant Difference (LSD) test and Duncan's test. The threshold for statistical significance was set at 95 % ($p < 0.05$), indicating the confidence level of the findings. For the graphical representation of the outcomes, Origin 2021 software was employed.

3. Results and discussion

3.1. Physical property analysis

3.1.1. Gel strength and TPA

Typically, gel strength serves as a key metric for assessing the quality of surimi products, indicating the gel-forming ability of proteins (Mi et al., 2021). As shown in Fig. 2, the gel strength of surimi gels with the addition of YG and OG (0.5 %–1.0 %) significantly increased ($p < 0.05$) compared to the control sample (0 % treated group). The gel strength of surimi gel reached maximin when adding 1.0 % YG or OG, 1124.27 g·mm and 1004.35 g·mm, respectively. The addition of β-glucan effectively promotes myosin unfolding, thus enhancing intermolecular hydrophobic interactions and functionally maintaining the gel structure, increasing the gel strength (Xu et al., 2022). When the β-glucan addition reached 1.5 %, the gel strength of surimi gel was significantly decreasing to 648.05 g·mm and 532.27 g·mm of YG and OG surimi gels, respectively. The introduction of excessive polysaccharides (YG and OG) produced obvious steric hindrance (S. Li et al., 2024), which could affect the gel network, leading to the reduction of surimi gel strength. When β-glucan from different sources was in the same amount, the quality of YG surimi gels was better than the samples with OG. It was due to the β-glucan from oat contains long, linear chains of β-(1 → 3) and β-(1 → 4) linkage between the glucose molecules. Cui et al. (2023) claimed that YG with branched chains could cause more friction and/or entanglement between molecules compared to OG, enhancing the gel properties. The higher gel strength of the YG surimi gel compared to the OG surimi gel could be attributed to this factor.

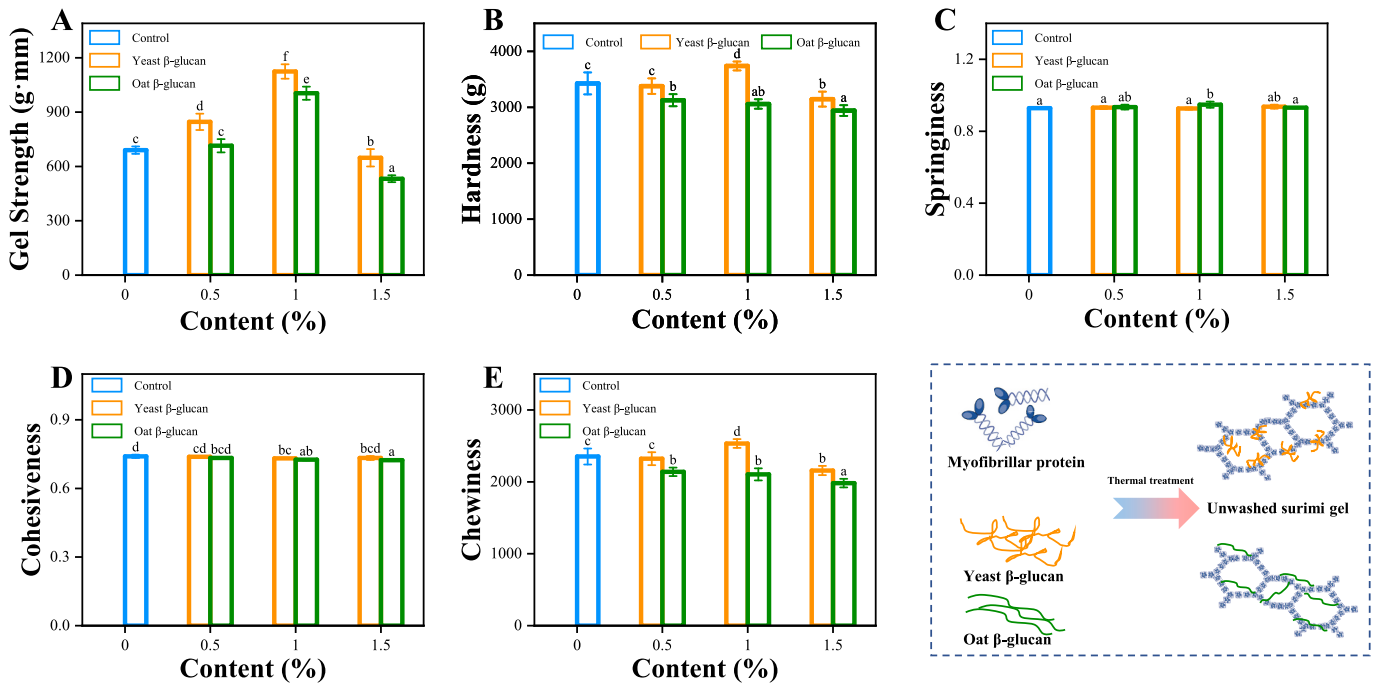

Fig. 2. Effect of YG or OG content on texture profile analysis of surimi gels.
Note: Different letters denote statistical significance ($p < 0.05$) among various treatments.

The TPA method is widely employed in various food applications to provide insights into the mechanical properties of foods under large-scale deformation, serving as an empirical approach for texture evaluation (Zhang et al., 2019). The hardness of surimi gel increased and then decreased with the increase of YG addition, and reached a maximum value of 3738.705 g when the YG addition reached 1.0 %. YG acts as a semi-rigid filler in MP and enhances the gel network structure, thus improving structural properties (Zhang et al., 2019). And the chewiness showed a similar trend. The textural properties of surimi gels weakened when both β-glucans were added at 1.5 %. It was evident that excessive amounts of β-glucan were detrimental to the cross-linking of proteins and the formation of gel networks. Zhang et al. (2019) found that β-glucan (0 % to 2 %) could improve the hardness, springiness, and chewiness of silver carp surimi, but the effect on cohesiveness was not significant. YG content above 2 %, resulted in the hardness, springiness, cohesiveness, and chewiness of surimi decreasing. The results suggest that appropriate addition of β-glucan can significantly improve the textural properties of gel samples, which was consistent with the results of gel strength. The differences in trends were observed for hardness and chewiness in the OG surimi gels compared to the gel strength. It could be due to changes in the gel's microstructure or the distribution of forces within the gel during the TPA test. Shen, Liu, Dong, Si and Li (2015) found the similar result.

3.1.2. *Rheological properties characterization*

Dynamic temperature sweep (*G'* and *G''* with temperature) were used to characterize the viscoelastic properties of surimi gels with 0 %–1.5 % β-glucan from different sources during heating. As shown in Fig. 3 and Fig. A.1, storage modulus *G'* and loss modulus *G''* of all samples show the great dependence on temperature. In detail, there was an inflection point at about 54 °C in all samples, which can be interpreted as a Modori (gel deterioration) phenomenon due to the degradation of the initial gel network by endogenous protein hydrolases (Fan et al., 2019). It remains relatively stable after reaching ~70 °C, indicating further gelation by protein unfolding and cross-linking under further heating and the formation of an irreversible and stable network structure (Zhu et al., 2024).

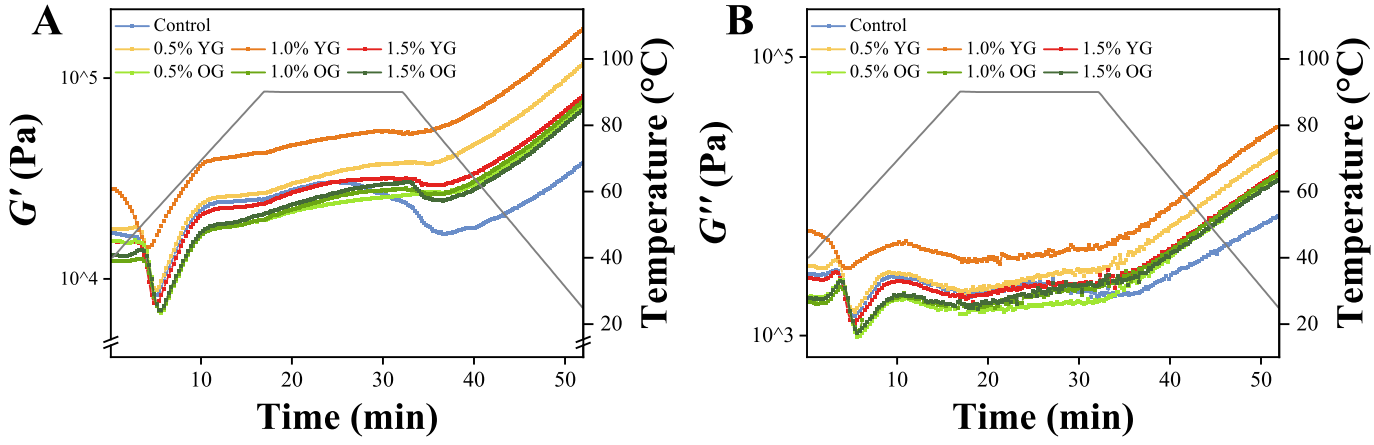

Fig. 3. Effect of YG or OG content on rheological properties of surimi gels: (A) storage modulus *G'*, (B) loss modulus *G''*.
Note: YG - the surimi gel with yeast β-glucan, OG - the surimi gel with oat β-glucan.

After the temperature has risen to 51.4 °C, the *G'* and *G"* values of YG and OG treated surimi gels were higher than that of control. This suggests that glucan plays a dominant role in thermotropic gelation through a filling effect and exerts an influence on the myofibrillar protein crosslink. The 1.0 % YG surimi gel displayed the high *G'* and *G"* value, relative to the other samples. The results showed that 1.0 % YG sample had the better protein crosslink density and therefore exhibited the best elastic properties, which matched the results of gel strength and TPA (Fig. 2). The addition of polysaccharides accelerated the unfolding of the protein structure and therefore enhanced the cross-linking of the proteins. He et al. (2023) and Yuan et al. (2019) also found that the addition of polysaccharides facilitated the formation of a tightly-ordered gel network, which improved the viscoelastic properties of the surimi gels. Moreover, the trihelical structure formed by YG could form aggregates, which had an impact on the rheological properties (Cui et al., 2023). The *G'* and *G"* of OG surimi gel were lower than those of the YG one. It indicated that YG with trihelical structures could cause more friction and/or entanglement between molecules in myofibrillar protein compared to OG.

3.2. The water retention analysis

3.2.1. Water holding capacity (WHC)

WHC is a critical quality attribute which indicates the bind water ability of the gel (Zhang et al., 2019). WHC of surimi gels with different contents of YG and OG are shown in Fig. 4A. With the increase of YG and OG additions (0 % to 1.0 %), the WHC of surimi gel increased from 97.77 % (control) to 98.69 % (1.0 % YG) and 98.67 % (1.0 % OG), respectively. This was due to the fact that the addition of β-glucan promoted the expansion of the protein structure, and the presence of hydroxyl groups in β-glucans facilitates hydrogen bonding with water (Edo et al., 2024). These contributed to the cross-linking and aggregation between the proteins, and the ordered and dense gel network structure provided more available space, leading to the locking of more water molecules in the gel network structure, and resulting in the improvement of the water holding capacity of the surimi gel samples (He et al., 2023).

However, the content of YG increased to 1.5 %, the WHC of surimi gel decreasing. Excessive YG can disrupt the three-dimensional protein network structure, leading to a compromised gel matrix integrity, a decline in the quality attributes of the food product (Cao et al., 2024). This may be related to $N_{exposed}$, which was able to participate in moderate or weak hydrogen bonding (Li et al., 2015). The $N_{exposed}$ value decreased from 66.67 % (1.0 % YG surimi gel) to 66.23 % (1.5 % YG surimi gel) as shown in Section 3.5.1. On the contrary, the WHC of 1.5 % OG sample was higher than that of 1.0 % OG sample. It could be due to the fact that the hydroxyl groups carried by OG can bind more water molecules through hydrogen bonding, preventing the loss of water molecules in the gel network structure under external forces (water bath thermal treatment), thus improving the water holding capacity (Geng et al., 2022). The $N_{exposed}$ value increased from 64.89 % (1.0 % OG surimi gel) to 65.78 % (1.5 % OG surimi gel). The balance between polysaccharides and proteins in surimi gels is a pivotal factor influencing protein aggregation, the appropriate ratio conducive to effective gel formation.

3.2.2. Low-field nuclear magnetic resonance (LF-NMR) analysis

The relaxation time (T_2) can reflect the fluidity and distribution of water molecules in surimi products by the degree of hydrogen proton restraint (Zhang et al., 2019). As shown in Fig. 4B and Table A.1, three distinct peaks centered at 0.2–2.3 ms (T_{2b}), 21–152 ms (T_{22}) and 231–933 ms (T_{23}) were observed in the surimi gels. The scales of the T_2 values represent the strength of the water fluidity. As the amount of β-glucan increased (0 % to 1.5 %), the initial relaxation time of T_{2b} was shortened to 0.66 ms and 0.60 ms for YG and OG surimi gels, respectively, compared with 0.94 ms of the control sample (Table A.1). T_{2b} represents bound water, which is closely associated with macromolecules by molecular force. The incorporation of β-glucan caused a leftward shift in the T_{2b} relaxation time of surimi gel, and an increase in the peak area, which suggests that the interaction between protein and water has become more stable (Ye et al., 2022). T_{22} corresponds to immobile water, which stays between the myofibrils and the membrane. T_{23} represents free water, which can freely motion and is located outside of the myofibrillar lattice (Zhang et al., 2019). It was worth noting that the immobile water (P_{22}) accounted for ~94 % of the total peak area to become the vast majority form of water in the surimi gels. Compared with the control sample, the addition of OG resulted in a decrease in the proportion of P_{23} and an increase in the proportion of P_{22} and P_{2b}. The addition of YG has a similar effect on OG surimi gel. The addition of YG and OG transferred the free water to the immobile water, formed a more regular and dense gel network, strengthened the binding of water molecules to the protein surface, and immobilized the free water in the gel matrix. Therefore, the addition of β-glucan can improve the water retention of surimi gels. In addition, due to the stronger water imbibition of OG that competed with protein for water, part of the bound water transformed into the immobile water, resulting in the P_{22} value of OG surimi gel more than YG surimi gel at the same content.

3.3. Grafting degree (GD) analysis

There are two main kinds of interactions between polysaccharides and proteins: covalent or noncovalent bonds (Gentile, 2020). The covalent bond is obtained through a Maillard-type reaction. This study analyzed the grafting degree of myofibrillar protein with β-glucan to assess whether a covalent interaction occurs between them. As shown in Fig. 5A, both YG and OG developed a concentration-dependent upward

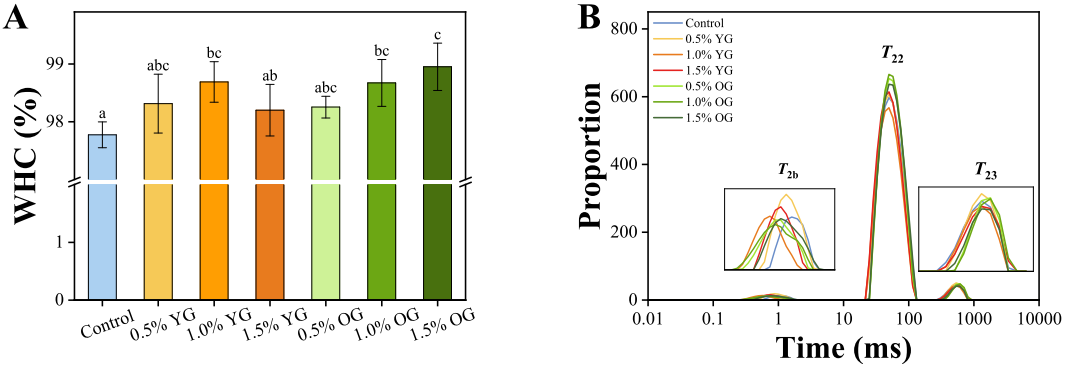

Fig. 4. Effect of YG or OG content on water holding capacity (WHC) (A), water distribution (B) of surimi gels.
Note: YG - the surimi gel with yeast β-glucan, OG - the surimi gel with oat β-glucan. Different letters denote statistical significance ($p < 0.05$) among various treatments.

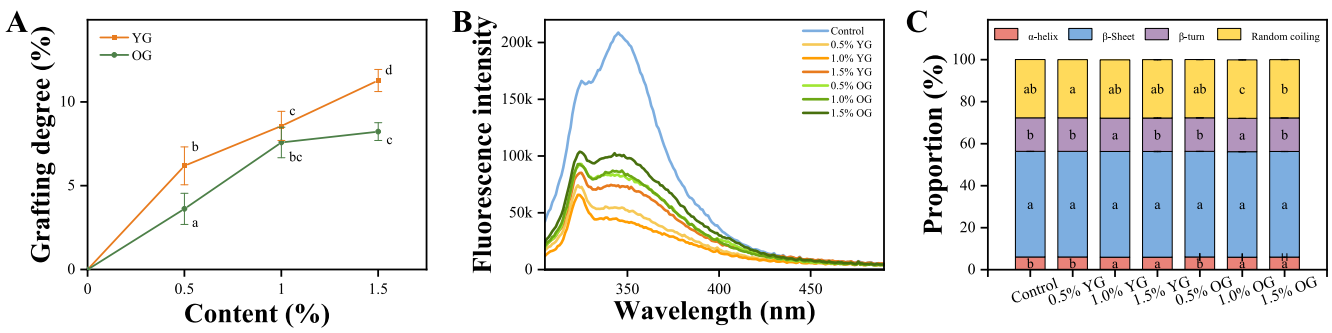

Fig. 5. Effect of YG or OG content on the grafting degree (GD) (A), intrinsic emission fluorescence spectroscopy (B), and secondary structure content (C) of surimi gels.

Note: YG - the surimi gel with yeast β-glucan, OG - the surimi gel with oat β-glucan. Different letters denote statistical significance ($p < 0.05$) among various treatments.

trend in grafting degree. Wang et al. (2024) also found that the grafting degree of the whey protein isolate (WPI)-*lycium barbarum* polysaccharide (LBP) complexes increase with the concentration of LBP (Wang et al., 2025). For the samples, when the β-glucan addition content was 1.5 %, the grafting degree of myofibrillar protein in the YG treated surimi was the highest (11.28 %) followed by those OG surimi gel (8.23 %). It has been claimed that the side chain of β-(1 → 6)-glucan could interact with other polymers flexibly, or as an attachment site to proteins (Zheng, Huang, Kang, Liu, & Luo, 2021). Both grafting degree and intrinsic fluorescence spectroscopy (Section 3.4.1) could reflect that the affinity of YG with myofibrillar protein was more than that of OG. Enhanced affinity improves the quality of surimi containing polysaccharides. However, the gel strength of the surimi gel with 1.5 % β-glucan was lower than 1.0 % sample. This was probably due to the higher degree of grafting could reduce the exposure of hydrophobic residues during the heating process of the protein, leading to the formation of a sparser structure and weak gel properties (Tang et al., 2022).

3.4. Spectral analysis

3.4.1. Intrinsic fluorescence spectra

To reveal the tertiary conformational changes in myofibrillar protein (MP) caused by β-glucan during heating, the intrinsic fluorescence emission spectra were recorded at an excitation wavelength of 285 nm to measure the environment surrounding tryptophan residues of the protein (Vetri & Militello, 2005). There were two peaks in the intrinsic fluorescence emission spectrum of control sample, at 325 nm and 345 nm, respectively (Fig. 5B). This is consistent with our previous research results (Xie, Zhao, et al., 2024). When Trp is located in a hydrophobic environment like being buried inside the protein or partitioned into the membrane, the emission peak experiences a significantly blue shift (~325–335 nm)(Brahma, Das, & Raghuraman, 2022). After the addition of β-glucan, there was a significant decrease in the fluorescence intensity of myofibrillar protein. It was speculated that the structure of myofibrillar protein was fully unfolded under ultrasound combined with β-glucan treatment, resulting in more aromatic amino acids being exposed and quenched in polar environment (Zhao et al., 2024). Moreover, due to the interaction between β-glucan and protein, which forms a more stable tertiary conformation in the protein so that tryptophan residues are embedded in hydrophobic molecules and blocked, leading to a decrease in fluorescence intensity. Therefore, β-glucan enhanced the gel structure of MP. Notably, the fluorescence intensity at $\lambda_{325\ nm}$ was higher than that at $\lambda_{345\ nm}$, which also indicated that β-glucan induced more Trp located in a hydrophobic environment. The effect of MP unfolding induced by YG could be stronger than OG, due to observing the fluorescence intensity of YG surimi gel lower than OG surimi gel. Raman spectroscopic analysis producing the same results, the degree of exposure of Trp residues of YG surimi gel was more than OG samples. This result suggested that YG induced more MP unfolding and promotes its cross-linking, which improved the hardness and gel strength of surimi gel.

3.4.2. Secondary structure analysis

In this research, the circular dichroism spectroscopy was utilized, which is a technique renowned for its sensitivity in detecting molecular-level alterations in protein conformation, as a non-destructive analytical tool (Hussain et al., 2024). As represented in Fig. 5C, control surimi gel contained 6.03 % as α-helix, 50.3 % β-sheet, 15.98 % β-turn and 27.75 % Random coiling. It was found that β-glucan had no significant effect on the secondary structure of myofibrillar protein. It is reported that the protein-hydrocolloids interactions were mainly electrostatic, between the positively charged groups on the protein and the anionic groups on the hydrocolloids (Mi et al., 2021). Due to the utilization of circular dichroism (CD) in this study, the measurement results only reflect the changes in the secondary structure of soluble proteins and do not fully represent the alterations in the protein of the surimi gel. This could account for the discrepancies observed between the protein structure and the grafting degree results. Pearson correlation analysis (depicted in Table A.2 and Table A.3.) revealed a significantly positive association between the α-helix content of YG surimi gel and cohesiveness ($r = 0.980$, $p < 0.05$, as shown in Table A.2). The correlation between the α-helix content and cohesiveness of OG surimi gel ($r = 0.818$, as shown in Table A.3) was lower than that of YG surimi gel sample. The results show that the effect of YG on the secondary structure of MP was more than OG, impacting on the physical properties of surimi gel.

3.5. Raman spectroscopic analysis

3.5.1. Tryptophan and tyrosine doublet

The normalized intensity at 760 cm^{-1} and 1003 cm^{-1} (I_{760}/I_{1003}) was used to monitor the degree of exposure of Trp residues (Wang, Guo, Zhao, & Feng, 2024). Table 1 shows the relative intensity of the Trp

Table 1
Tyrosine doublet ratio I_{850}/I_{830}, tryptophan ration I_{760}/I_{1003}, and O—H stretching band of I_{3220}/I_{3400} results in unwashed surimi gel.

Sample	I_{850}/I_{830}	I_{760}/I_{1003}	I_{3220}/I_{3400}
Control	0.99 ± 0.00^{a}	0.97 ± 0.01^{c}	0.87 ± 0.00^{a}
0.5 % YG	1.00 ± 0.02^{a}	0.96 ± 0.01^{bc}	0.92 ± 0.01^{b}
1.0 % YG	1.00 ± 0.00^{a}	0.93 ± 0.02^{a}	1.00 ± 0.02^{c}
1.5 % YG	1.00 ± 0.02^{a}	0.92 ± 0.01^{a}	1.02 ± 0.03^{c}
0.5 % OG	1.01 ± 0.04^{a}	0.91 ± 0.03^{a}	0.92 ± 0.02^{b}
1.0 % OG	0.99 ± 0.02^{a}	0.94 ± 0.02^{abc}	0.98 ± 0.01^{c}
1.5 % OG	0.99 ± 0.01^{a}	0.93 ± 0.02^{ab}	0.99 ± 0.02^{c}

Note: YG - the surimi gel with yeast β-glucan, OG - the surimi gel with oat β-glucan. Different letters denote statistical significance ($p < 0.05$) among various treatments within the same column.

residues of surimi gel with 0 %–1.5 % YG or OG. The I_{760}/I_{1003} ratio decreased from 0.97 (Control sample) to 0.92 (1.5 % YG surimi gel) and 0.93 (1.5 % OG surimi gel). The decrease in the I_{760}/I_{1003} ratio was induced by the addition of β-glucan, indicating that the unfolding of the protein structure treated by under ultrasound combined with β-glucan. This is consistent with the results of intrinsic fluorescence emission spectra.

The relative intensity Raman bands of I_{850}/I_{830} reflect the nature of hydrogen bonding and the state of the phenolic hydroxyl groups in the tyrosine (Tyr) side chains (Xie et al., 2022). As depicted in Table 1, the I_{850}/I_{830} ratios of all surimi gels ranged from 0.90 to 1.01, evincing that tyrosine residues were predominately exposed to get involved in moderate or weak hydrogen bonding with water molecules (Wang et al., 2023). The percentages of exposed *vs.* buried tyrosine residues were calculated according to the I_{850}/I_{830} value (as shown in Fig. 6 B, C). The $N_{exposed}$ value increased from 64.44 % (Control sample) to 66.23 % (1.5 % YG surimi gel) and 65.78 % (1.5 % OG surimi gel). The incorporation of β-glucan into the unwashed surimi gel led to a slight exposure of tyrosine residues to the polar aqueous environment, facilitating the ability to form hydrogen bonds with water molecules (Xie et al., 2022), improving the WHC of the surimi gel (as shown in Fig. 4A).

3.5.2. *O—H stretching*

Water molecules exhibit vibrations that encompass two distinct O—H stretching frequencies: a symmetric vibration peaking at approximately 3220 cm^{-1} and an asymmetric vibration peaking near 3400 cm^{-1} (Sánchez-González et al., 2008). As shown Table 1, the I_{3220}/I_{3400} value of β-glucan surimi sample which was higher than that of control one. The higher value of I_{3220}/I_{3400}, the smaller the water domain sizes. The larger interstitial water domain could trap more water in the gel matrix (Liu, Zhao, Xie, & Xiong, 2011), correspond with higher WHC of the β-glucan treated groups.

3.6. *Chemical interaction force*

The changes in the soluble protein content that is ionic bonds, hydrogen bonds, hydrophobic interactions, and disulfide bonds of surimi gels treated with β-glucan were determined as reported method previously (Xie et al., 2024), and the results are shown in Fig. 6A. In this research, the hydrophobic interactions and disulfide bonds in surimi were the main chemical interaction forces in the surimi gel. β-glucan was remarkably influenced the hydrophobic interactions in the surimi gel, which is consistent with previous reports. Generally, exposure to heat prompts the unfolding of myofibrillar protein helical structures, leading to the increased exposure of sulfhydryl groups and hydrophobic amino acids. This exposure facilitates the formation of disulfide bonds and enhances hydrophobic interactions (Huang et al., 2024). The hydrophobic interactions gradually increased with the increase of YG and OG contents, and the maximum values were reached in surimi gels containing 1.0 % added YG and OG (3.77 mg/mL, 3.29 mg/mL). However, the content of YG and OG increased to 1.5 %, the hydrophobicity in the surimi gel decreased (3.68 mg/mL, 3.24 mg/mL). The increase in β-glucan led to a gradual increase in water absorption, and water molecules in surimi gels could be retained within a certain range, enhancing texture properties of surimi gel. This is consistent with the results of Section 3.1.1. However, the multiple degrees of water absorption hindered the dispersion or solubilization of the protein itself in water, thus affecting the hydrophobic interactions in the system to a certain extent. Among them, the hydrophobic interaction of OG surimi gel was weaker than that of YG surimi gel. YG is branched β-(1 → 3),(1 → 6)-glucans and with the trihelical structure, whereas OG is a linear β-(1 → 3),(1 → 4)-glucans (Cui et al., 2023). The β-(1 → 6)-glycosidic side chains contribute to receptor binding by increasing the available contact surface area and enhancing flexibility, while β-(1 → 4)-glycosidic linkages restricted available binding sites with other molecules (Huo et al., 2025). It could be speculated that YG promoted the hydrophobic interaction formation between myofibrillar protein, improving the quality of surimi gel through comprehensive analysis. What's more, hydrogen bond content also was significantly increased in β-glucan treated samples (Fig. 6A, $p < 0.05$), but there was no significant difference between YG and OG surimi gels. A negative association between the hydrogen bond content of YG surimi gel and cohesiveness ($r = -0.993$, $p < 0.01$, as shown in Table A.2), while a much weaker correlation between the hydrogen bond content and cohesiveness of OG surimi gel ($r = -0.458$, as shown in Table A.3). This result is mutually verified by molecular docking (Section 3.7), exhibiting that YG has a stronger ability to bind MHC through hydrogen bonds than OG. The addition of β-glucan significantly increased the disulfide bond ($p < 0.05$), indicating that it could increase the covalent cross-linking between MP and further maintain the network structure of the MP gel (Zhao et al., 2024).

3.7. *Analysis of the binding mode of β-glucan and MHC*

Molecular docking techniques aim to predict the binding modes and affinities between molecules, which was employed to investigate the binding patterns of MHC with β-glucans in this research (Roche, Brackenridge, & McGuffin, 2015). The CDOCKER energy of YG-MHC and OG-MHC were 23.173 kcal/mol and 57.996 kcal/mol, respectively. It is recognized that a lower CDOCKER energy value corresponds to a more stable binding mode between proteins and polysaccharides (S. Li et al., 2024). Compared to OG, the more stable the binding mode between MHC and YG, which may be due to the greater physical properties of the YG surimi gel. As the gel strength and TPA results shown that the gel strength and hardness of the YG treated surimi gel were higher than that of OG one at the same addition levels (Section 3.1.1). In addition, due to the tighter binding of YG with MHC compared to OG, the average pore size of YG treated surimi gel were lower than that of OG

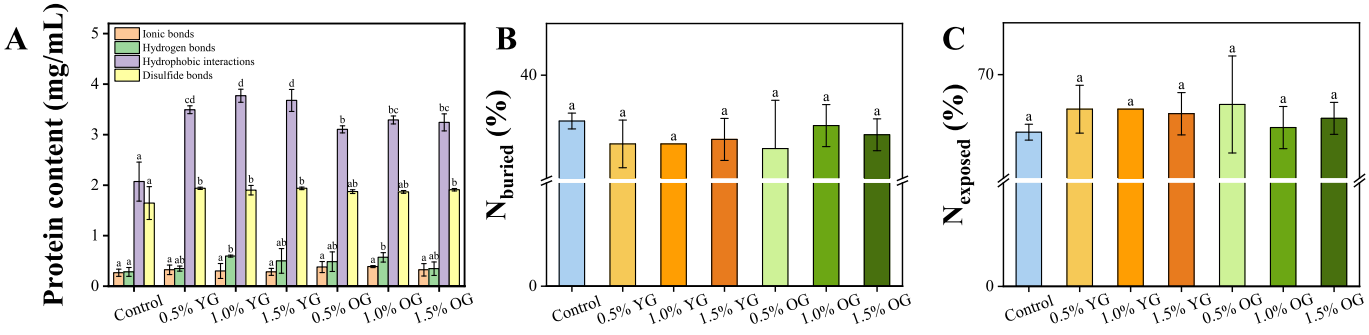

Fig. 6. Effect of YG or OG content on the intermolecular interactions (A), the molar fractions of buried (B) and exposed (C) tyrosine residues of surimi gels.
Note: YG - the surimi gel with yeast β-glucan, OG - the surimi gel with oat β-glucan. Different letters denote statistical significance ($p < 0.05$) among various treatments.

one at the same addition level. The surface and bonding interface of YG or OG and MHC for the active site were shown in Fig. 7. The main force of YG and MHC was hydrogen bond, which is consistent with the results studied by Wang, Wang, Luo, Zhang, and Cao (2019). YG could form conventional hydrogen bonding interactions with Lys-191, Lys-130, Glu-187, Asn-235, Asn-127, Gly-182 and Phe-129 in the active site of MHC, and carbon hydrogen bonding interactions with Arg-131, Pro-128, Asn-233, and Gly-184 in the active site of MHC (Figure 7Ac). Furthermore, OG could form conventional hydrogen bonding interactions with Lys-190, Asn-127, Asn-233, Glu-187, Lys-191, and Lys-130 in the active site of MHC, and carbon hydrogen bonding interactions with Pro-128 and Asn-235 in the active site of MHC (Figure 7Bc). The formation of hydrogen bonds was crucial for the anchoring of small molecules in the protein pocket (Gao, Hu, Wang, Ahmad, & Zhu, 2023). The number of hydrogen bonds between YG of protein was more than that of OG, which can be supported for the results of Section 3.6 Interaction Force. YG with a branched-chain structure has a stronger interaction with myofibrillar protein, which could contribute to enhance the stability of protein-polysaccharide complex gel. Hydrogen bonds formed between MHC and β-glucans can enhance the overall network stability and contribute to the rigidity of the gel structure. These bonds can complement the hydrophobic interactions and disulfide bonds, leading to a more robust gel network (Cao et al., 2024). YG can form stronger hydrogen bonds with proteins compared to OG, resulting in improved gelation properties.

3.8. Microstructure of surimi gels

3.8.1. Light microscopy

The spatial distribution of two kinds of β-glucan in the surimi gels was shown by the paraffin section with HE staining, observed through light microscopy (40× and 100×) (Fig. 8A). The phase behavior of polysaccharides in composite gels is mainly manifested in two forms: one is trapped in the MP gel network, which is the backbone structure, with the polysaccharides as uniformly dispersed particulate fillers; the other is interpenetrating with the MP gel network, with both the polysaccharides and the MP gel network being the main structure (Zhuang, Wang, Jiang, Chen, & Zhou, 2020). It can be seen that the control surimi gel forms a relatively loose gel network structure, with many uncolored and fibriform cracks observed. There were many circular cavities in the 0.5 % YG sample, and trapped in the MP three-dimensional gel networks. As the amount of YG increased, the circular cavities became progressively larger and took up more area. It is supposed that the phase behavior of YG in the surimi gels is the backbone structure, improving the physical properties of protein gel. Upon the incorporation of 1.5 % YG, the circular cavities dimensions become excessively expansive, having a negative impact on the myofibrillar protein (MP) network. This alteration in the network structure could potentially diminish the mechanical properties of the surimi gel. Zhang et al. (2019) observed that the addition of less than 2 % YG enhanced the structural integrity of surimi as a semirigid filler. In contrast, a 5 % YG incorporation induced significant structural defects and porosity, impairing gel continuity. OG had similar phase behavior in the MP gel networks than that of YG. The OG was in irregular shape and trapped in the MP gel networks. It could be due to the fact that OG is a linear chain polysaccharide.

3.8.2. CLSM

Fluorescence confocal laser scanning microscopy (CLSM) was used to signify differences in the microstructure of the samples (Fig. 8B), the spatial distribution of proteins and polysaccharides in the confocal laser scanning microscopy images was determined by coloring the green (Nile blue) and the blue (Calcofluor white). The distribution of the protein network matrix in the control surimi gel was smooth. The addition of β-glucan produced tight aggregates in the protein matrix and the proteins gradually aggregated from small dispersed protein clusters into larger ones, which contributed to the increase in WHC and gel strength

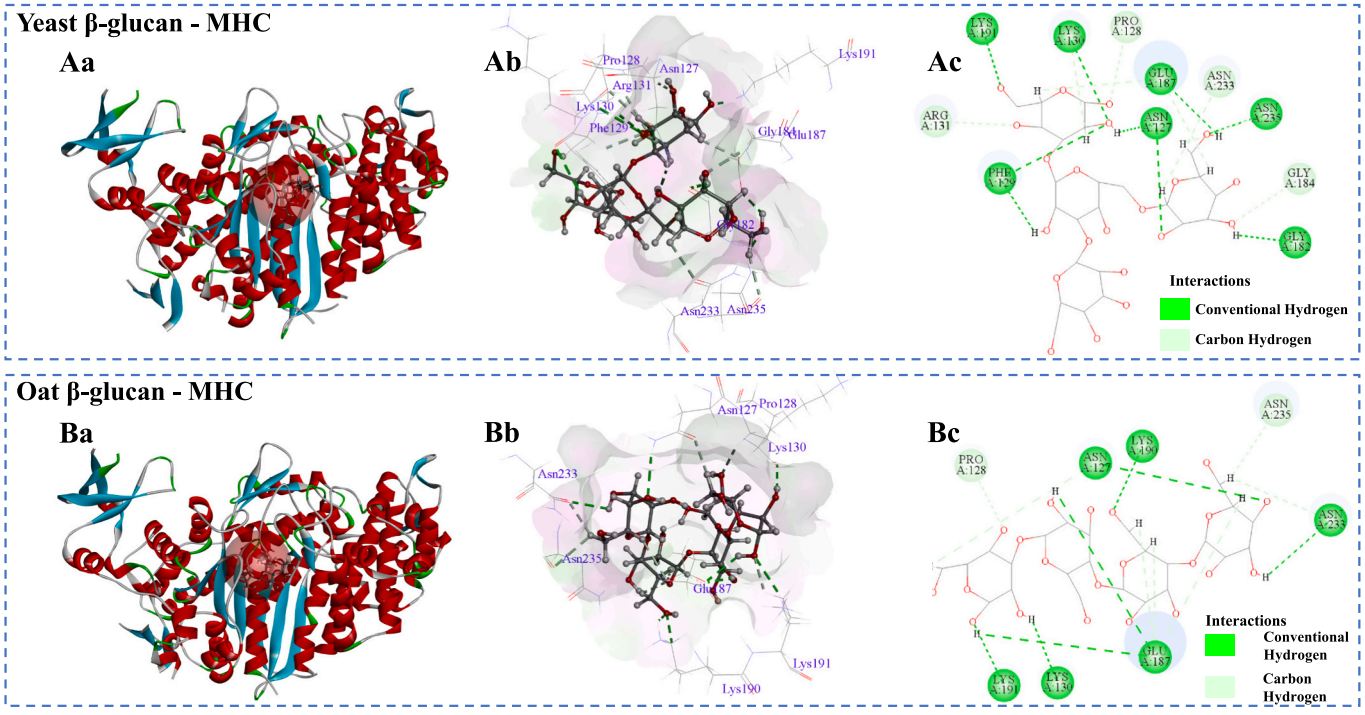

Fig. 7. Molecular docking of the interactions of MHC and β-glucan (a). The complex of MHC and β-glucan (b). The residues on protein interact with β-glucan (c). The 2D diagrams of MHC and β-glucan interaction. A represents YG. B represents peptide OG.
Note: YG - the surimi gel with yeast β-glucan, OG - the surimi gel with oat β-glucan.

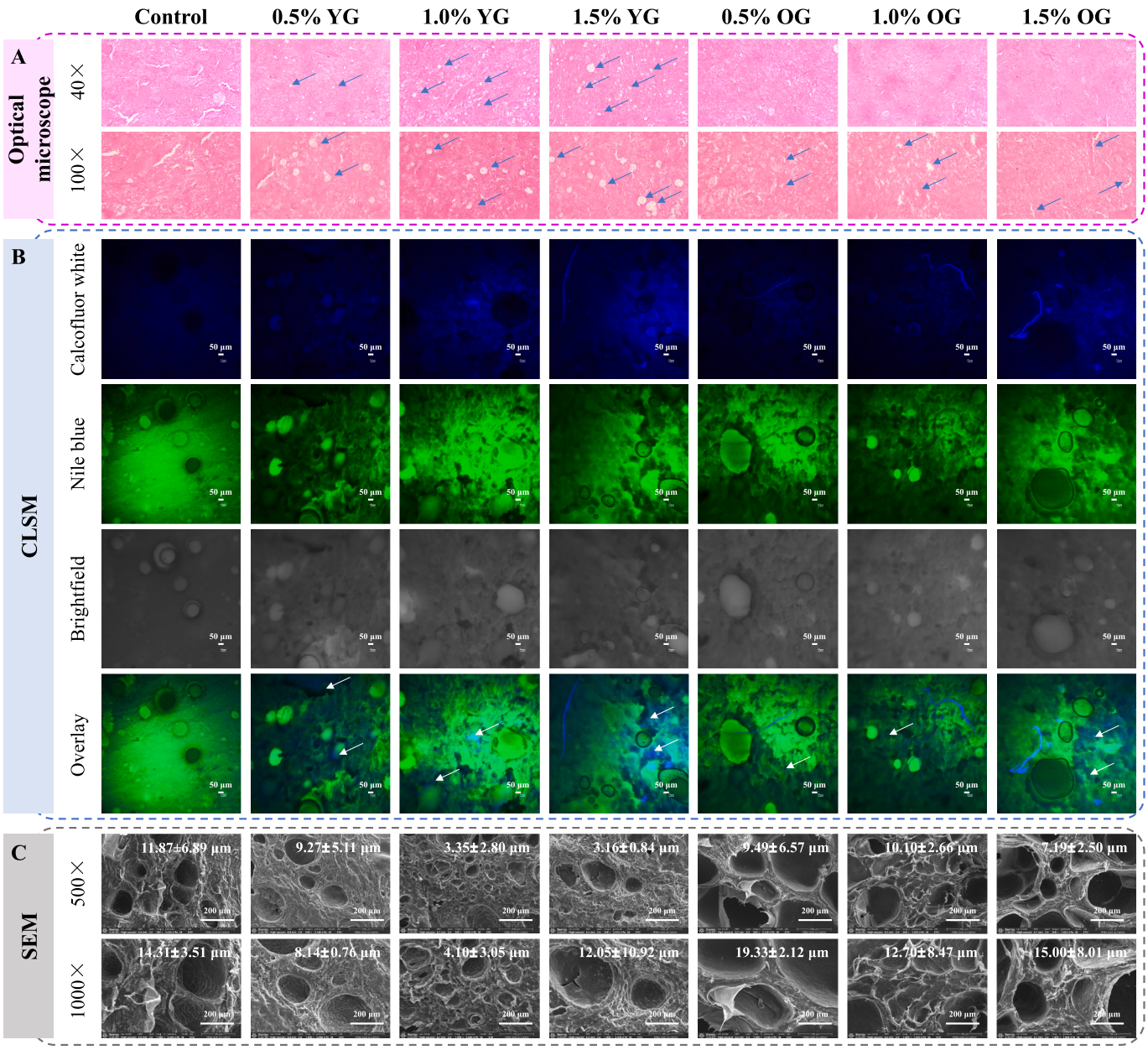

Fig. 8. Micrograph images of surimi gel with different content of YG or OG: the light micrographs images (A), confocal laser scanning microscopy (CLSM) images (B), scanning electron microscopy images (C), and the average pore sizes (inset).
Note: YG - the surimi gel with yeast β-glucan, OG - the surimi gel with oat β-glucan.

(X. Wang et al., 2024). The covalent linking, hydrogen bonding and electrostatic interactions between proteins and β-glucan, previously deduced from GD analysis and chemical interaction force results, were verified in the CLSM images by the density of the overlap of green and blue fluorescence (Niu, Yu, Xue, Xue, & Mao, 2024). Compared with OG samples, the fluorescence overlay area in YG was greater, indicating interactions between proteins and YG higher than that of OG.

3.8.3. SEM

Fig. 8C shows the microstructure of surimi gel with 0 % to 1.5 % of YG or OG. The microstructure was observed with 500× and 1000× magnification. The structure of the control surimi gel is loose and rough, with uneven pore size and irregular distribution, and divided into several aggregated areas with a large number of "water channels" (Han et al., 2022). The average pore size of three SEM images was calculated from the cavities counts for lacunarity measurements and the partial area corresponding to cavities (Dàvila et al., 2007), as exemplified in Fig. 8C inset. Compared with the average pore size of control (14.31 μm at 1000×), the microstructure of the composite gel with added β-glucan was denser and less porous. At the same magnification, the average pore sizes of 1.0 % YG surimi gel was decreasing to 4.10 μm, and 1.0 % OG surimi gel reached 12.70 μm. β-glucan forms hydrogen bonds with water molecules inside proteins through hydroxyl groups (J. Li et al., 2024), significantly reduced the pore sizes, and the gel structure became dense and ordered. In surimi gel, YG with trihelix structure is stabilized by forming stronger hydrogen bonds with MHC compared to OG (Section 3.7), and YG surimi gel forming compact network. As the added amount β-glucan increased, more pores were formed and extension, and the continuous structure of the myofibrillar protein was gradually destroyed (Cao et al., 2024), resulting in the decreasing gel strength.

4. Conclusion

The study investigated the mechanisms by which the addition of YG and OG at levels ranging from 0 % to 1.5 % affected the quality of unwashed surimi gel. β-glucan could induce more unfolding and promoted cross-linking of myofibrillar protein, leading to the higher hardness and gel strength of unwashed surimi gel, at the addition of 0.5 % and 1.0 %. Upon the incorporation of 1.5 % YG or OG, more pores were formed and extension, having a negative impact on the myofibrillar protein network. Both grafting degree and intrinsic fluorescence spectroscopy reflected that the affinity of YG with myofibrillar protein was more than that of OG. The molecular docking analysis further proved it, and the number of hydrogen bonds between YG of protein was more than that of OG. Lower CDOCKER energy of YG-MHC, and the phase behavior of YG in the surimi gels is the backbone structure, resulting the physical properties of YG treated group greater than OG treated group. The addition of YG with a branched-chain structure serves as an efficacious strategy to enhance the myofibrillar protein (MP) network, consequently ameliorating the quality of unwashed surimi-based products. This study lies in its comprehensive investigation of the interactions between myofibrillar proteins and β-glucans, elucidating the mechanisms by which these interactions improve gelation properties. This work has laid a solid foundation for understanding the complex relationships between protein and polysaccharide components in food systems, which is essential for the innovation of new protein-polysaccharide food products.

The present study did not investigate the potential mixture of YG and OG in relation to the gel properties of surimi gel, nor did it explore the synergistic effect of β-glucan and ultrasound treatment on the MP structure. These aspects merit comprehensive examination in the ration of YG:OG and the synergistic application of ultrasound treatment in the future.

CRediT authorship contribution statement

Yisha Xie: Writing – original draft, Supervision, Investigation, Funding acquisition. **Kangyu Zhao:** Writing – original draft, Methodology, Formal analysis, Data curation. **Jing Peng:** Investigation, Data curation. **Li Jiang:** Investigation, Data curation. **Wenjing Shu:** Investigation. **Yizhen Huang:** Writing – review & editing. **Qingqing Liu:** Writing – review & editing, Visualization. **Wei Luo:** Software. **Yongjun Yuan:** Resources, Funding acquisition, Formal analysis.

Declaration of competing interest

The authors declare that they have no known competing financial interests or personal relationships that could have appeared to influence the work reported in this paper.

Acknowledgments

This work was supported by Sichuan Science and Technology Program [grant number 2024NSFSC1253], key technologies for the improve of “Tianfu rapeseed oil” processing [grant number 2023TFRO05]. Acknowledgments to the College of Biological Science and Engineering of Fuzhou University for providing software of molecular docking support.

Appendix A. Supplementary data

Supplementary data to this article can be found online at https://doi.org/10.1016/j.foodres.2025.116248.

Data availability

Data will be made available on request.

References

Bai, J., Ren, Y., Li, Y., Fan, M., Qian, H., Wang, L., Wu, G., Zhang, H., Qi, X., Xu, M., & Rao, Z. (2019). Physiological functionalities and mechanisms of β-glucans. *Trends in Food Science & Technology, 88*, 57–66. https://doi.org/10.1016/j.tifs.2019.03.023

Brahma, R., Das, A., & Raghuraman, H. (2022). Site-directed fluorescence approaches to monitor the structural dynamics of proteins using intrinsic Trp and labeled with extrinsic fluorophores. *STAR Protocols, 3*(1), Article 101200. https://doi.org/10.1016/j.xpro.2022.101200

Cao, H., Li, R., Shi, M., Song, H., Li, S., & Guan, X. (2024). Promising effects of β-glucans on gelation in protein-based products: A review. *International Journal of Biological Macromolecules, 256*, Article 127574. https://doi.org/10.1016/j.ijbiomac.2023.127574

Cui, Y., Han, X., Huang, X., Xie, W., Zhang, X., Zhang, Z., Yu, Q., Tao, L., Li, T., & Li, S. (2023). Effects of different sources of β-glucan on pasting, gelation, and digestive properties of pea starch. *Food Hydrocolloids, 135*, Article 108172. https://doi.org/10.1016/j.foodhyd.2022.108172

Dàvila, E., Toldrà, M., Saguer, E., Carretero, C., & Parés, D. (2007). Characterization of plasma protein gels by means of image analysis. *LWT - Food Science and Technology, 40*(8), 1321–1329. https://doi.org/10.1016/j.lwt.2006.10.004

Edo, G. I., Ndudi, W., Makia, R. S., Ainyanbhor, I. E., Yousif, E., Gaaz, T. S., … Umar, H. (2024). Beta-glucan: An overview in biological activities, derivatives, properties, modifications and current advancements in food, health and industrial applications. *Process Biochemistry, 147*, 347–370. https://doi.org/10.1016/j.procbio.2024.09.011

Fan, M., Huang, Q., Zhong, S., Li, X., Xiong, S., Xie, J., Yin, T., Zhang, B., & Zhao, S. (2019). Gel properties of myofibrillar protein as affected by gelatinization and retrogradation behaviors of modified starches with different crosslinking and acetylation degrees. *Food Hydrocolloids, 96*, 604–616. https://doi.org/10.1016/j.foodhyd.2019.05.045

Gao, Y., Hu, Y., Wang, J., Ahmad, H. N., & Zhu, J. (2023). Modification of low-salt myofibrillar protein using combined ultrasound pre-treatment and konjac glucomannan for improving gelling properties: Intermolecular interaction and filling effect. *International Journal of Biological Macromolecules, 250*, Article 126195. https://doi.org/10.1016/j.ijbiomac.2023.126195

Geng, H., Sun, W., Zhan, S., Jia, R., Lou, Q., & Huang, T. (2024). Glycosylation with different saccharides on the gelling, rheological and structural properties of fish gelatin. *Food Hydrocolloids, 150*, Article 109699. https://doi.org/10.1016/j.foodhyd.2023.109699

Geng, X., Zhao, N., Song, X., Wu, J., Zhu, Q., Wu, T., … Zhang, M. (2022). Fabrication and characterization of Konjac Glucomannan/oat β-glucan composite hydrogel: Microstructure, physicochemical properties and gelation mechanism studies. *Molecules, 27*(23), 8494. https://doi.org/10.3390/molecules27238494

Gentile, L. (2020). Protein-polysaccharide interactions and aggregates in food formulations. *Current Opinion in Colloid & Interface Science, 48*, 18–27. https://doi.org/10.1016/j.cocis.2020.03.002

Gore, S. B., Balange, A. K., Nayak, B. B., Kumar, H. S., Tandale, A. T., & Xavier, K. A. M. (2022). Comparative analysis of unwashed and single washed mince gel from Indian major carps. *Journal of Food Science and Technology, 59*(1), 377–387. https://doi.org/10.1007/s13197-021-05024-5

Han, K., Li, S., Yang, Y., Feng, X., Tang, X., & Chen, Y. (2022). Mechanisms of inulin addition affecting the properties of chicken myofibrillar protein gel. *Food Hydrocolloids, 131*, Article 107843. https://doi.org/10.1016/j.foodhyd.2022.107843

He, X., Lv, Y., Li, X., Yi, S., Zhao, H., Xu, Y., & Li, J. (2023). Effect of oat *β*-glucan on gel properties and protein conformation of silver carp surimi. *Journal of the Science of Food and Agriculture, 103*(7), 3367–3375. https://doi.org/10.1002/jsfa.12525

Huang, X., Liu, Q., Wang, P., Song, C., Ma, H., Hong, P., & Zhou, C. (2024). Tapioca starch improves the quality of *Virgatus nemipterus* surimi gel by enhancing molecular interaction in the gel system. *Foods, 13*(1), 169. https://doi.org/10.3390/foods13010169

Huo, R., Wuhanqimuge, Z., & M., Sun, M., & Miao, Y.. (2025). Molecular dynamics modeling of different conformations of beta-glucan, molecular docking with dectin-1, and the effects on macrophages. *International Journal of Biological Macromolecules, 293*, Article 139382. https://doi.org/10.1016/j.ijbiomac.2024.139382

Hussain, A., Hussain, M., Ashraf, W., Karim, A., Muhammad Aqeel, S., Khan, A., Hussain, A., Khan, S., & Lianfu, Z. (2024). Preparation, characterization and functional evaluation of soy protein isolate-peach gum conjugates prepared by wet heating Maillard reaction. *Food Research International, 192*, Article 114681. https://doi.org/10.1016/j.foodres.2024.114681

Jayachandran, M., Chen, J., Chung, S. S. M., & Xu, B. (2018). A critical review on the impacts of β-glucans on gut microbiota and human health. *The Journal of Nutritional Biochemistry, 61*, 101–110. https://doi.org/10.1016/j.jnutbio.2018.06.010

Shen, R.-l., Liu, X.-y., Dong, J.-l., Si, J.-l., & Li, H. (2015). The gel properties and microstructure of the mixture of oat β-glucan/soy protein isolates. Food Hydrocolloids, 47, 108–114. doi:https://doi.org/10.1016/j.foodhyd.2015.01.017.

Li, J., An, N., Ren, G., Wang, L., Chen, N., Sun, J., … Dong, J. (2024). Effect of plant polysaccharides on the conformation and gel properties of the eugenol-Myofibrillar protein complex. *Food Bioscience, 59*, Article 104041. https://doi.org/10.1016/j.fbio.2024.104041

Li, J., Munir, S., Yu, X., Yin, T., You, J., Liu, R., Xiong, S., & Hu, Y. (2021). Double-crosslinked effect of TGase and EGCG on myofibrillar proteins gel based on physicochemical properties and molecular docking. *Food Chemistry, 345*, Article 128655. https://doi.org/10.1016/j.foodchem.2020.128655

Li, K., Zhao, Y. Y., Kang, Z. L., Wang, P., Han, M. Y., Xu, X. L., & Zhou, G. H. (2015). Reduced functionality of PSE-like chicken breast meat batter resulting from

alterations in protein conformation. *Poultry Science, 94*(1), 111–122. https://doi.org/10.3382/ps/peu040

Li, S., Lin, S., Jiang, P., Bao, Z., Qian, X., Wang, S., & Sun, N. (2024). The interaction mechanism of different ionic polysaccharides with myofibrillar protein and its contribution to the heat-induced gels. *Food Frontiers, 5*(4), 1613–1628. https://doi.org/10.1002/fft2.403

Liu, R., Wang, N., Li, Q., & Zhang, M. (2015). Comparative studies on physicochemical properties of raw and hydrolyzed oat β-glucan and their application in low-fat meatballs. *Food Hydrocolloids, 51*, 424–431. https://doi.org/10.1016/j.foodhyd.2015.04.027

Liu, R., Zhao, S.-M., Xie, B.-J., & Xiong, S.-B. (2011). Contribution of protein conformation and intermolecular bonds to fish and pork gelation properties. *Food Hydrocolloids, 25*(5), 898–906. https://doi.org/10.1016/j.foodhyd.2010.08.016

Mi, H., Li, Y., Wang, C., Yi, S., Li, X., & Li, J. (2021). The interaction of starch-gums and their effect on gel properties and protein conformation of silver carp surimi. *Food Hydrocolloids, 112*, Article 106290. https://doi.org/10.1016/j.foodhyd.2020.106290

Niu, Z., Yu, J., Xue, Y., Xue, C., & Mao, X. (2024). Synergistic effects and interactions among components in the surimi/κ-carrageenan/soybean oil system. *Food Hydrocolloids, 156*, Article 110250. https://doi.org/10.1016/j.foodhyd.2024.110250

Rahar, S., Swami, G., Nagpal, N., Nagpal, M., & Singh, G. (2011). Preparation, characterization, and biological properties of β-glucans. *Journal of Advanced Pharmaceutical Technology & Research, 2*(2), 94–103. https://doi.org/10.4103/2231-4040.82953

Roche, D. B., Brackenridge, D. A., & McGuffin, L. J. (2015). Proteins and Their Interacting Partners: An Introduction to Protein–Ligand Binding Site Prediction Methods. International Journal of Molecular Sciences, 16(12), 29829–29842. doi: https://doi.org/10.3390/ijms161226202.

Sánchez-González, I., Carmona, P., Moreno, P., Borderías, J., Sánchez-Alonso, I., Rodríguez-Casado, A., & Careche, M. (2008). Protein and water structural changes in fish surimi during gelation as revealed by isotopic H/D exchange and Raman spectroscopy. *Food Chemistry, 106*(1), 56–64. https://doi.org/10.1016/j.foodchem.2007.05.067

Shen, X., Li, T., Li, X., Wang, F., Liu, Y., & Wu, J. (2022). Dual cryoprotective and antioxidant effects of silver carp (*Hypophthalmichthys molitrix*) protein hydrolysates on unwashed surimi stored at conventional and ultra-low frozen temperatures. *LWT - Food Science and Technology, 153*, Article 112563. https://doi.org/10.1016/j.lwt.2021.112563

Sujithra, S., Arthanareeswaran, G., Ismail, A. F., & Taweepreda, W. (2024). Isolation, purification and characterization of β-glucan from cereals - a review. *International Journal of Biological Macromolecules, 256*, Article 128255. https://doi.org/10.1016/j.ijbiomac.2023.128255

Tang, S., Jiang, Y., Tang, T., Du, H., Tu, Y., & Xu, M. (2022). Effects of grafting degree on the physicochemical properties of egg white protein-sodium Carboxymethylcellulose conjugates and their aerogels. *Applied Sciences, 12*(4), 2017. https://doi.org/10.3390/app12042017

Vannucci, L., Krizan, J., Sima, P., Stakheev, D., Caja, F., Rajsiglova, L., Horak, V., & Saieh, M. (2013). Immunostimulatory properties and antitumor activities of glucans. *International Journal of Oncology, 43*(2), 357–364. https://doi.org/10.3892/ijo.2013.1974

Vetri, V., & Militello, V. (2005). Thermal induced conformational changes involved in the aggregation pathways of beta-lactoglobulin. *Biophysical Chemistry, 113*(1), 83–91. https://doi.org/10.1016/j.bpc.2004.07.042

Walayat, N., Wei, R., Su, Z., Lorenzo, J. M., & Nawaz, A. (2024). Effect of tea polysaccharides on fluctuated frozen storage impaired total sulfhydryl level and structural attributes of silver carp surimi proteins. *Food Hydrocolloids, 157*, Article 110448. https://doi.org/10.1016/j.foodhyd.2024.110448

Wang, H., Zhang, J., Rao, P., Zheng, S., Li, G., Han, H., Chen, Y., & Xiang, L. (2025). Mechanistic insights into the interaction of *Lycium barbarum* polysaccharide with whey protein isolate: Functional and structural characterization. *Food Chemistry, 463*, Article 141080. https://doi.org/10.1016/j.foodchem.2024.141080

Wang, Q., Luan, Y., Tang, Z., Li, Z., Gu, C., Liu, R., Ge, Q., Yu, H., & Wu, M. (2023). Consolidating the gelling performance of myofibrillar protein using a novel OSA-modified-starch-stabilized Pickering emulsion filler: Effect of starches with distinct crystalline types. *Food Research International, 164*, Article 112443. https://doi.org/10.1016/j.foodres.2022.112443

Wang, R., Guo, F., Zhao, J., & Feng, C. (2024). Myofibril degradation and structural changes in myofibrillar proteins of porcine longissimus muscles during frozen storage. *Food Chemistry, 435*, Article 137671. https://doi.org/10.1016/j.foodchem.2023.137671

Wang, X., Li, M., Shi, T., Monto, A. R., Yuan, L., Jin, W., & Gao, R. (2024). Enhancement of the gelling properties of *Aristichthys nobilis*: Insights into intermolecular interactions between okra polysaccharide and myofibrillar protein. *Current Research in Food Science, 9*, Article 100814. https://doi.org/10.1016/j.crfs.2024.100814

Wang, Y., Wang, Y., Luo, Q., Zhang, H., & Cao, J. (2019). Molecular characterization of the effects of Ganoderma Lucidum polysaccharides on the structure and activity of bovine serum albumin. *Spectrochimica Acta Part A: Molecular and Biomolecular Spectroscopy, 206*, 538–546. https://doi.org/10.1016/j.saa.2018.08.051

Xie, Y., Yang, F., Shu, W., Zhao, K., Huang, Y., Liu, Q., & Yuan, Y. (2024). Improved qualities of cod-rice dual-protein gel as affected by rice protein: Insight into molecular flexibility, protein interaction and gel properties. *Food Research International, 197*, Article 115176. https://doi.org/10.1016/j.foodres.2024.115176

Xie, Y., Yu, X., Wang, Y., Yu, C., Prakash, S., Zhu, B., & Dong, X. (2022). Role of dietary fiber and flaxseed oil in altering the physicochemical properties and 3D printability of cod protein composite gel. *Journal of Food Engineering, 327*, Article 111053. https://doi.org/10.1016/j.jfoodeng.2022.111053

Xie, Y., Zhao, K., Yang, F., Shu, W., Ma, J., Huang, Y., … Yuan, Y. (2024). Modification of myofibrillar protein structural characteristics: Effect of ultrasound-assisted first-stage thermal treatment on unwashed silver carp surimi gel. *Ultrasonics Sonochemistry, 107*, Article 106911. https://doi.org/10.1016/j.ultsonch.2024.106911

Xu, Y., Lv, Y., Yin, Y., Zhao, H., Li, X., Yi, S., & Li, J. (2022). Improvement of the gel properties and flavor adsorption capacity of fish myosin upon yeast β-glucan incorporation. *Food Chemistry, 397*, Article 133766. https://doi.org/10.1016/j.foodchem.2022.133766

Yang, Y., Jiao, A., Liu, Q., Ren, X., Zhu, K., & Jin, Z. (2022). The effects of removing endogenous proteins, β-glucan and lipids on the surface microstructure, water migration and glucose diffusion *in vitro* of starch in highland barley flour. *Food Hydrocolloids, 127*, Article 107457. https://doi.org/10.1016/j.foodhyd.2021.107457

Ye, Y., Liu, X., Bai, W., Zhao, W., Zhang, Y., Dong, H., & Pan, Z. (2022). Effect of microwave-ultrasonic combination treatment on heating-induced gel properties of low-sodium tilapia surimi during gel setting stage and comparative analysis. *LWT - Food Science and Technology, 161*, Article 113386. https://doi.org/10.1016/j.lwt.2022.113386

Yuan, L., Yu, J., Mu, J., Shi, T., Sun, Q., Jin, W., & Gao, R. (2019). Effects of deacetylation of konjac glucomannan on the physico-chemical properties of surimi gels from silver carp (*Hypophthalmichthys molitrix*). *RSC Advances, 9*(34), 19828–19836. https://doi.org/10.1039/C9RA03517F

Zhang, H., Xiong, Y., Bakry, A. M., Xiong, S., Yin, T., Zhang, B., … Huang, Q. (2019). Effect of yeast β-glucan on gel properties, spatial structure and sensory characteristics of silver carp surimi. *Food Hydrocolloids, 88*, 256–264. https://doi.org/10.1016/j.foodhyd.2018.10.010

Zhang, T., Zhang, L., Yin, T., You, J., Liu, R., Huang, Q., Shi, L., Wang, L., Liao, T., Wang, W., & Ma, H. (2023). Recent understanding of stress response on muscle quality of fish: From the perspective of industrial chain. *Trends in Food Science & Technology, 140*, Article 104145. https://doi.org/10.1016/j.tifs.2023.104145

Zhang, Y., Bai, G., Wang, Y., Wang, J., Teng, W., Li, M., Yao, X., & Cao, J. (2025). Exploring the potential of fibrinogen hydrolysates as enhancers for myofibrillar protein gelation: Insights into molecular assembly behavior. *Food Chemistry, 464*, Article 141587. https://doi.org/10.1016/j.foodchem.2024.141587

Zhang, Y., Lyu, H., Wang, Y., Bai, G., Wang, J., Teng, W., Wang, W., & Cao, J. (2024). Optimizing the formation of myosin/high-density lipoprotein composite gels: PH-dependent effects on heat-induced aggregation. *International Journal of Biological Macromolecules, 268*, Article 131786. https://doi.org/10.1016/j.ijbiomac.2024.131786

Zhao, H., He, X., Lv, Y., Xu, Y., Yi, S., Li, J., & Li, X. (2024). Thermal aggregation behavior of silver carp myofibrillar protein at low salt content: Effect of oat β-glucan combined with ultrasound-assisted heating. *Food Chemistry, 455*, Article 139903. https://doi.org/10.1016/j.foodchem.2024.139903

Zheng, Z., Huang, Q., Kang, Y., Liu, Y., & Luo, W. (2021). Different molecular sizes and chain conformations of water-soluble yeast β-glucan fractions and their interactions with receptor Dectin-1. *Carbohydrate Polymers, 273*, Article 118568. https://doi.org/10.1016/j.carbpol.2021.118568

Zhu, S., Wang, Y., Ding, Y., Xiang, X., Yang, Q., Wei, Z., Song, H., Liu, S., & Zhou, X. (2024). Improved texture properties and toughening mechanisms of surimi gels by double network strategies. *Food Hydrocolloids, 152*, Article 109900. https://doi.org/10.1016/j.foodhyd.2024.109900

Zhuang, X., Wang, L., Jiang, X., Chen, Y., & Zhou, G. (2020). The effects of three polysaccharides on the gelation properties of myofibrillar protein: Phase behaviour and moisture stability. *Meat Science, 170*, Article 108228. https://doi.org/10.1016/j.meatsci.2020.108228

Zhuang, X., Wang, L., Jiang, X., Chen, Y., & Zhou, G. (2021). Insight into the mechanism of myofibrillar protein gel influenced by konjac glucomannan: Moisture stability and phase separation behavior. *Food Chemistry, 339*, Article 127941. https://doi.org/10.1016/j.foodchem.2020.127941